TOXICOLOGICAL SCIENCES **127(2)**, 438–450 (2012)
doi:10.1093/toxsci/kfs133
Advance Access publication April 5, 2012

Liver-Specific Loss of Atg5 Causes Persistent Activation of Nrf2 and Protects Against Acetaminophen-Induced Liver Injury

Hong-Min Ni, Nikki Boggess, Mitchell R. McGill, Margitta Lebofsky, Prachi Borude, Udayan Apte, Hartmut Jaeschke, and Wen-Xing Ding[1]

Department of Pharmacology, Toxicology and Therapeutics, University of Kansas Medical Center, Kansas City, Kansas 66160

[1]To whom correspondence should be addressed at Department of Pharmacology, Toxicology and Therapeutics, University of Kansas Medical Center, MS 1018, 3901 Rainbow Boulevard, Kansas City, KS 66160. Fax: (913) 588-7501. E-mail: wxding@kumc.edu.

Received December 20, 2011; accepted March 20, 2012

Autophagy is an evolutionarily conserved biological process that degrades intracellular proteins and organelles including damaged mitochondria through the formation of autophagosome. We have previously demonstrated that pharmacological induction of autophagy by rapamycin protects against acetaminophen (APAP)-induced liver injury in mice. In contrast, in the present study, we found that mice with the liver-specific loss of Atg5, an essential autophagy gene, were resistant to APAP-induced liver injury. Hepatocyte-specific deletion of Atg5 resulted in mild liver injury characterized by increased apoptosis and compensatory hepatocyte proliferation. The lack of autophagy in the Atg5-deficient mouse livers was confirmed by increased p62 protein levels and the absence of LC3-lipidation as well as autophagosome formation. Analysis of histological and clinical chemistry parameters indicated that the Atg5 liver–specific knockout mice are resistant to APAP overdose (500 mg/kg). Further investigations revealed that the bioactivation of APAP is normal in Atg5 liver–specific knockout mice although they had lower CYP2E1 expression. There was an increased basal hepatic glutathione (GSH) content and a faster recovery of GSH after APAP treatment due to persistent activation of Nrf2, a transcriptional factor regulating drug detoxification and GSH synthesis gene expression. In addition, we found significantly higher hepatocyte proliferation in the livers of Atg5 liver–specific knockout mice. Taken together, our data suggest that persistent activation of Nrf2 and increased hepatocyte proliferation protect against APAP-induced liver injury in Atg5 liver–specific knockout mice.

Key Words: **acetaminophen; autophagy; Atg5; liver injury.**

Acetaminophen (APAP) overdose can cause liver injury and even liver failure in animals (Mitchell *et al*., 1973) and in humans (Larson *et al*., 2005). APAP-induced liver injury involves the formation of a reactive metabolite (N-acetyl-*p*-benzoquinone imine, NAPQI), which depletes glutathione (GSH) and binds to cellular proteins (Mitchell *et al*., 1973). Therefore, the intracellular GSH levels are a critical factor in the pathophysiology. In fact, one of the most effective antidotes against APAP hepatotoxicity is N-acetylcysteine (NAC), which acts as a prodrug for GSH synthesis (Corcoran *et al*., 1985). In addition to the detoxification of NAPQI, GSH has also been shown to scavenge reactive oxygen species and peroxynitrite and support the mitochondrial energy metabolism (Knight *et al*., 2002).

During the last decade, mitochondrial dysfunction and oxidant stress emerged as the most critical events in APAP-mediated liver cell death (Jaeschke and Bajt, 2006; Jaeschke *et al*., 2003). APAP overdose causes inhibition of the mitochondrial respiratory chain (Meyers *et al*., 1988), selective mitochondrial reactive oxygen (Jaeschke, 1990) and peroxynitrite formation (Cover *et al*., 2005), mitochondrial translocation of bax (Bajt *et al*., 2008), and activated c-jun-N-terminal kinase (Hanawa *et al*., 2008), which further promotes the mitochondrial oxidant stress (Saito *et al*., 2010) and eventually triggers the mitochondrial membrane permeability transition pore opening resulting in the collapse of the membrane potential and necrotic cell death (Kon *et al*., 2004). As the extent of mitochondrial damage determines APAP-induced cell death, it is not unexpected that APAP overdose triggers autophagy as a defense mechanism to remove damaged mitochondria (Ni *et al*., 2012). Most importantly, pharmacological stimulation of autophagy with rapamycin protects against APAP-induced hepatotoxicity (Ni *et al*., 2012).

Macroautophagy (hereafter referred to as autophagy) is a process in which cytoplasmic components are degraded by the autolysosome. Autophagy is a tightly regulated and highly inducible process, which involves the formation of double-membrane autophagosomes (Mizushima *et al*., 2008). Autophagosomes enwrap cytoplasm and organelles and then fuse with lysosomes to form matured autolysosomes and degrade the enveloped contents. The formation of double membrane autophagosomes involves two ubiquitin-like conjugation systems including the formation of Atg12-Atg5-Atg16 complex, which is mediated by Atg7 (E1-like) and Atg10 (E2-like) proteins, and the conjugation of microtubule-associated protein

light chain 3 (LC3), a mammalian homologue of yeast *Atg*8, with phosphatidylethanolamine (PE), which is mediated by Atg7 (E1-like) and Atg3 (E2-like) proteins. The PE-conjugated form of LC3 (LC3-II) translocates to the autophagosomal membrane and promotes the formation a double membrane autophagosome, whereas the unconjugated LC3 resides in the cytosol (LC3-I) (Ohsumi and Mizushima, 2004). Systemic Atg5- or Atg7-knockout mice die after birth likely due to the lack of nutrients as a result of loss of autophagy during the neonatal period (Komatsu *et al*., 2005; Kuma *et al*., 2004). Mice with the systemic mosaic deletion of Atg5, in which only 10–40% of cells have the deletion of Atg5, develop spontaneous benign tumors in the liver (Takamura *et al*., 2011). Mice with liver-specific deletion of Atg7 develop severe hepatomegaly, with increased accumulation of ubiquitin and p62-positive aggregates and have developed benign liver tumors (Inami *et al*., 2011). Moreover, it has also been suggested that increased p62 in the Atg7-deficient mouse liver leads to persistent activation of nuclear factor (erythroid-derived 2)-like 2 (Nrf2) by releasing Kelch-like ECH-associated protein 1 (Keap1) from Nrf2, resulting in the nuclear translocation of Nrf2. Activation of Nrf2 increases the expression of many detoxification and antioxidant genes and paradoxically increases liver injury in the Atg7-deficient mouse liver (Komatsu *et al*., 2010). Therefore, autophagy is generally thought to act as a survival mechanism in response to an adverse environment as well as a tumor suppressor (Mizushima *et al*., 2008).

We and others have clearly demonstrated that APAP induces necrosis, but not apoptosis, in C57Bl/6 mouse liver, in primary cultured mouse hepatocytes, and in human HepRG cells expressing cytochrome P450 2E1 (CYP2E1) to metabolize APAP (McGill *et al*., 2011; Ni *et al*., 2012). We also demonstrated that pharmacological induction of autophagy by rapamycin almost completely inhibits APAP-induced liver injury (Ni *et al*., 2012). Therefore, our goal in the present study was to assess APAP-induced liver injury using a genetic autophagy–deficient mouse model.

MATERIALS AND METHODS

Antibodies. Antibodies used in the study were p62 (Abnova), β-actin (Sigma), Atg5, cleaved caspase-3, glyceraldehyde 3-phosphate dehydrogenase (Cell Signaling), NAD(P)H dehydrogenase quinone 1 (NQO1), CYP2E1 (Abcam), glutamate-cysteine ligase catalytic subunit (GCLC), and glutamate-cysteine ligase modifier subunit (GCLM) were kindly provided by Dr Terry Kavanagh (University of Washington, Seattle, WA), proliferating cell nuclear antigen (PCNA) (Santa Cruz and Cell Signaling). The rabbit polyclonal anti-LC3 antibody was described previously (Ding *et al*., 2009). The secondary antibodies used in this study were horseradish peroxidase (HRP)-conjugated goat anti-mouse or rabbit antibodies (Jackson ImmunoResearch).

Animal experiments. Atg5 Flox/Flox mice (C57BL/6/129) were generated by Dr N. Mizushima as described previously (Hara *et al*., 2006) and were crossed with Albumin-Cre mice (Alb-Cre, C57BL/6) (Jackson Laboratory). All animals received humane care. All procedures were approved by the Institutional Animal Care and Use Committee of the University of Kansas Medical Center. Male Alb-Cre-positive Atg5 Flox/Flox mice and the Alb-Cre-negative Atg5 Flox/Flox–matched littermates were given either saline ($n = 5$, ip) or APAP (500 mg/kg) ($n \geq 3$, ip). Mice were sacrificed at 0.5, 2, 6, and 24 h after APAP treatment. Liver injury was assessed by the determination of the serum alanine aminotransferase (ALT) activities and hematoxylin and eosin (HE) staining of liver sections as we described previously (Mei *et al*., 2011; Ni *et al*., 2012). Caspase-3 activities were determined using fluorescent substrates Ac-DEVD-AFC (Biomol) as we described previously (Ding *et al*., 2004). Total liver lysates were prepared using RIPA buffer (1% NP40, 0.5% sodium deoxycholate, 0.1% sodium dodecyl [lauryl] sulfate).

Immunoblot assay. Twenty micrograms of liver lysates from each sample was separated by SDS-polyacrylamide gel electrophoresis and transferred to polyvinylidene fluoride membranes. The membranes were stained with primary antibodies followed by secondary HRP-conjugated antibodies. The membranes were further developed with SuperSignal West Pico chemiluminescent substrate (Pierce).

Electron microscopy. For electron microscopy (EM), liver tissues were fixed with 2.5% glutaraldehyde in 0.1 mol/l phosphate buffer (pH 7.4), followed by 1% OsO_4. After dehydration, thin sections were stained with uranyl acetate and lead citrate for observation under a JEM 1011CX electron microscope (JEOL, Peabody, MA). Images were acquired digitally. The average number of autophagosomes from each cell was determined from a randomly selected pool of 15–20 fields under each condition.

PCNA staining. Immunohistochemical detection of PCNA was done on paraffin-embedded liver tissue sections as previously described (Wolfe *et al*., 2011).

Terminal deoxynucleotidyl transferase dUTP nick end labeling assay. Terminal deoxynucleotidyl transferase dUTP nick end labeling (TUNEL) assay was performed with In Situ Cell Death Detection Kit from Roche following the manufacturer's instruction. Briefly, cryopreserved liver tissue sections were permeabilized with 0.1% Triton X-100 followed by staining in terminal deoxynucleotidyl transferase and fluorescein label solution mixture. Nuclei were stained with Hoechst 33342 (1 μg/ml).

Real-time PCR. RNA was isolated from mouse livers using TRIzol (Invitrogen) and reverse transcribed into complementary DNA by RevertAid Reverse Transcriptase (Fermentas). Real-time PCR was used to quantify Nrf2, Keap1, NQO1, GCLC, GCLM, and β-actin and performed on an Applied Biosystems Prism 7900HT Real-Time PCR instrument (ABI, Foster City, CA) using Maxima SYBR Green/Rox qPCR reagents (Fermentas). The sequences of the primers were as follows: β-actin forward: 5′-TGT TAC CAA CTG GGA CGA CA- 3′, β-actin reverse: 5′-GGG GTG TTG AAG GTC TCA AA-3′; NQO1 forward: 5′- CAG ATC CTG GAA GGA TGG AA-3′, NQO1 reverse: 5′-TCT GGT TGT CAG CTG GAA TG-3′; GCLC forward: 5′-AAC ACA GAC CCA CAA ACC CAG AG-3′, GCLC reverse: 5′-CCG CAT CTT CTG GAA ATG TT-3′; GCLM forward: 5′-TGT GTG ATG CCA CCA GAT TT-3′, GCLM reverse: 5′-GAT GAT TCC CCT GCT CTT CA-3'; Nrf2 forward: 5′-CGA GAT ATA CGC AGG AGA GGT AAG A-3', Nrf2 reverse: 5′-GCT CGA CAA TGT TCT CCA GCT T-3′; Keap1 forward 5′-AAG GAA CAT GAT ATG CCC TGA CA-3′, Keap1 reverse: 5′-ACA CAG GCC GGC TCC AT-3′; tumor necrosis factor (TNF)-α forward: 5′-CGT CAG CCG ATT TGC TAT CT-3′, TNF-α reverse: 5′-CGG ACT CCG CAA AGT CTA AG-3'; IL-6 forward: 5′-ACA ACC ACG GCC TTC CCT ACT T-3′, IL-6 reverse: 5′-CAT TTC CAC GAT TTC CCA GAG A-3′.

Hepatic GSH content and APAP-protein adducts measurement. GSH was measured using a modified Tietze assay, as described (Jaeschke, 1990). APAP-cysteine (APAP-Cys) adducts were measured by high-pressure liquid chromatography with electrochemical detection according to the method of Muldrew *et al*. (2002) with minor differences. Namely, sample dialysis was replaced with a rapid gel-filtration method to remove free APAP and APAP-GSH prior to digestion and analysis. Protein levels were determined using a standard bicinchoninic acid assay, and adducts were normalized to total protein in the liver homogenates.

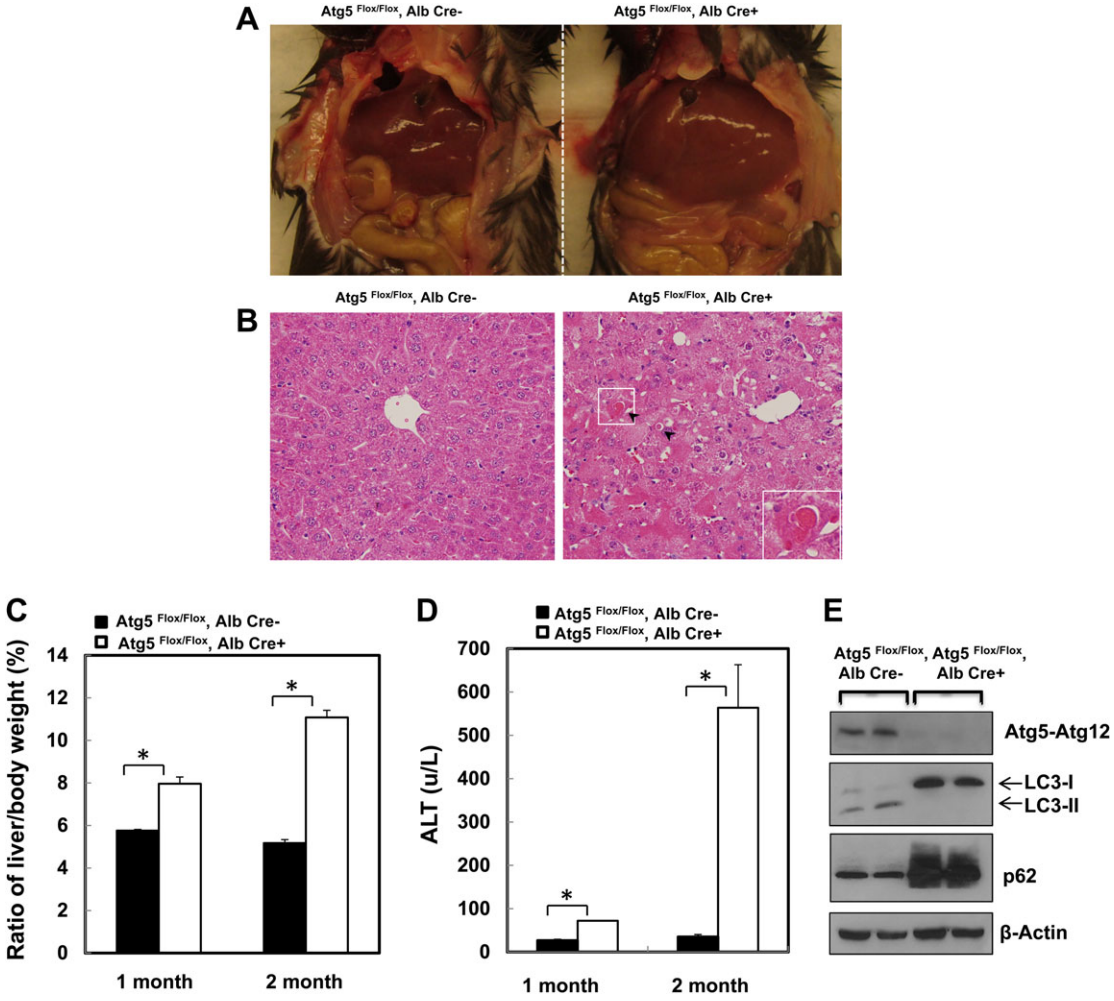

FIG. 1. Loss of Atg5 in the mouse liver leads to hepatomegaly and liver injury. (A) The gross anatomical views of representative mouse liver from 2-month-old Cre-negative and Cre-positive Atg5 Flox/Flox mouse. (B) Representative photographs of HE staining are presented. Arrows: apoptotic cells. Inserted: enlarged image from the squared area. (C) Ratio of the liver to body weight and (D) serum ALT levels from 1- to 2-month-old Cre-negative and Cre-positive Atg5 Flox/Flox mouse. Data are means ± SE ($n = 3$). *$p < 0.05$ Student's *t*-test. (E) Total liver lysates from 2-month-old Cre-negative and Cre-positive Atg5 Flox/Flox mouse were subjected to Western blot analysis.

Statistical analysis. Experimental data were subjected to Student's *t*-test or one-way ANOVA analysis with Scheffé's *post hoc* test where appropriate.

RESULTS

Loss of Atg5 in the Liver Leads to Hepatomegaly and Liver Injury

It has been previously reported that loss of Atg7 in the liver leads to hepatomegaly and liver injury when Atg7 was deleted by using Mx1Cre and ip injection of pIpC (Komatsu *et al.*, 2005, 2010). Similar to the loss of Atg7, here we found that loss of Atg5 in the liver by using Alb-Cre also led to hepatomegaly and liver injury. As can be seen, the liver to body weight ratio increased almost 50% in 1-month-old Alb-Cre-positive Atg5 Flox/Flox mice, and it was increased almost twofold in 2-month-old Alb-Cre-positive Atg5 Flox/Flox mice when compared with their wild-type littermates (Figs. 1A and 1C). Histological examination of Alb-Cre-positive and -negative mouse livers showed increased apoptotic cells (Fig. 1B, arrows) and the appearance of enlarged hepatocytes (megalocytosis) in Alb-Cre-positive mouse livers (Fig. 1B). Moreover, serum ALT levels, a widely used marker to monitor liver injury, increased significantly in the Alb-Cre-positive Atg5 Flox/Flox mice, suggesting increased liver injury as a result of loss of Atg5 in the mouse liver (Fig. 1D). Western blot analysis confirmed the deletion of Atg5, loss of PE-conjugated LC3 form (LC3-II), as well as elevated p62 levels in Alb-Cre-positive Atg5 Flox/Flox mouse liver (Fig. 1E), indicating the loss of autophagy in the mouse liver.

Atg5 Liver-Specific Knockout Mice Are Resistant to APAP-Induced Liver Injury

We previously demonstrated that activation of autophagy by rapamycin suppresses APAP-induced hepatotoxicity *in vitro*

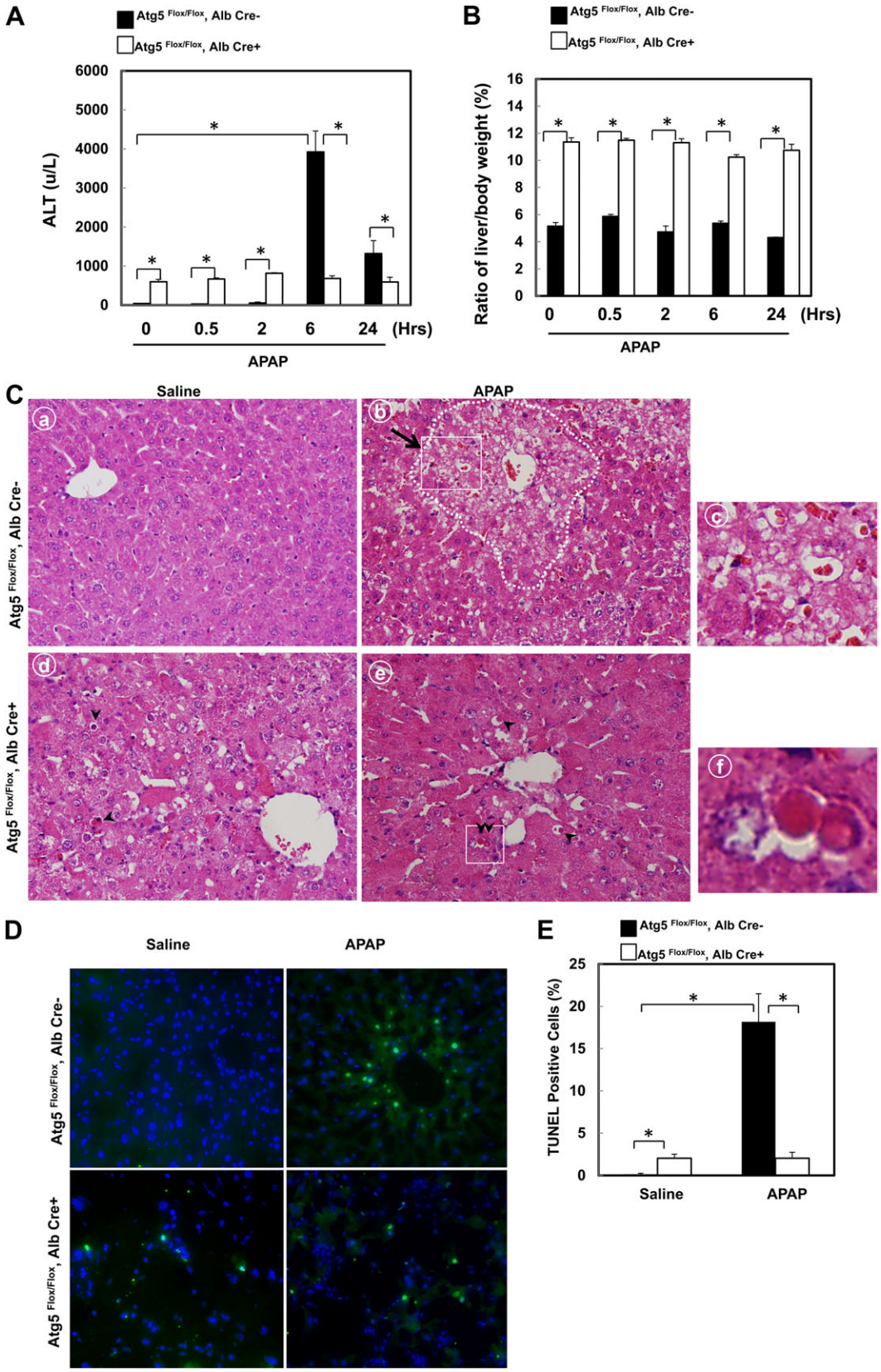
A
Atg5 Flox/Flox, Alb Cre-
Atg5 Flox/Flox, Alb Cre+
ALT (u/L)
6000
5000
4000
3000
2000
1000
0
0 0.5 2 6 24 (Hrs)
APAP
B
Atg5 Flox/Flox, Alb Cre-
Atg5 Flox/Flox, Alb Cre+
Ratio of liver/body weight (%)
16
14
12
10
8
6
4
2
0
0 0.5 2 6 24 (Hrs)
APAP
C
Saline
APAP
Atg5 Flox/Flox, Alb Cre-
Atg5 Flox/Flox, Alb Cre+
a
b
c
d
e
f
D
Saline
APAP
Atg5 Flox/Flox, Alb Cre-
Atg5 Flox/Flox, Alb Cre+
E
Atg5 Flox/Flox, Alb Cre-
Atg5 Flox/Flox, Alb Cre+
TUNEL Positive Cells (%)
25
20
15
10
5
0
Saline
APAP

and *in vivo* (Ni *et al*., 2012). We thus hypothesized that APAP would increase liver injury in Atg5 liver–specific knockout mice. We found that APAP significantly increased serum ALT levels in Alb-Cre-negative Atg5 Flox/Flox mice after 6 and 24 h treatment, which is in agreement with previous reports (Fig. 2A) (Ni *et al*., 2012; Saito *et al*., 2010). The decreasing ALT levels after 24-h treatment with APAP compared with 6 h indicates that the injury process is completed well before 24 h. Although the ALT levels were already higher in control Atg5 liver–specific knockout mice (Alb-Cre-positive Atg5 Flox/Flox mice) compare with the matched wild-type littermates control, ALT levels remained almost the same level in Atg5 liver–specific knockout mice regardless of APAP treatment at all the time points that we assessed, which were remarkably lower than that of APAP-treated wild-type mice (Fig. 2A). Although the liver/body weight ratio was already higher in the nontreated Atg5 liver–specific knockout mice, there was no change in the liver/body weight ratio after APAP treatment in both Atg5 liver–specific knockout mice and matched wild-type mice (Fig. 2B). Histological analysis revealed typical centrilobular necrosis as demonstrated by cellular vacuolization, cell swelling, and nuclear disintegration in APAP-treated wild-type mice liver (Fig. 2C, panels b and c, arrow). In contrast, necrotic cell death was almost undetectable in APAP-treated Atg5 liver–specific knockout mice. Interestingly, increased apoptotic cells were readily detected as demonstrated by the cell shrinkage and nuclear condensation in the control Atg5 liver–specific knockout mouse liver, and the apoptotic cell death nature was not altered after APAP treatment (Fig. 2C, panels d–f, arrow heads). We previously demonstrated that APAP-induced necrotic cells had increased DNA fragmentation as indicated by the TUNEL assay (Saito *et al*., 2010). Indeed, we found that the number of TUNEL-positive cells was significantly increased in APAP-treated Alb-Cre-negative Atg5 Flox/Flox mice, and most of the TUNEL-positive cells were located in the centrilobular areas where most necrotic cells were found in HE-stained sections (Fig. 2D). In contrast, although there was an increased basal level of TUNEL-positive cells in the Alb-Cre-positive Atg5 Flox/Flox mouse liver, which were not restricted to the centrilobular areas, no significant changes were observed after treatment with APAP for 6 h (Figs. 2D and 2E). These results indicate that APAP-induced necrotic cell death was significantly blocked in mouse livers with loss of Atg5.

Defects of Autophagy and Increased Caspase-3 Activation in Atg5 Liver–Specific Knockout Mice

We next determined the effects of APAP on autophagy in both Alb-Cre-negative and -positive Atg5 Flox/Flox mice. APAP treatment increased the levels of LC3-II in Alb-Cre-negative Atg5 Flox/Flox mouse liver (Fig. 3A). As expected, no LC3-II proteins were detected in APAP-treated Alb-Cre-positive Atg5 Flox/Flox mouse livers. Although the p62 levels were increased in Alb-Cre-positive Atg5 Flox/Flox mouse livers compared with Alb-Cre-negative Atg5 Flox/Flox mouse livers, APAP treatment did not further alter the p62 levels (Fig. 3A). EM studies revealed that autophagosome structures were readily detected in the hepatocytes of APAP-treated Alb-Cre-negative Atg5 Flox/Flox mouse livers (Fig. 3B, panel b, arrows), which is consistent with our previous report (Ni *et al*., 2012). However, no typical autophagosomal structures were detected in the hepatocytes of Alb-Cre-positive Atg5 Flox/Flox mouse livers either with or without APAP treatment (Fig. 3B, panels c and d). Similar to the Atg7 liver–specific knockout mice (Komatsu *et al*., 2005), many aberrant multimembrane structures, which often surrounded multiple number of lipid droplets, were readily detected in Alb-Cre-positive Atg5 Flox/Flox mouse liver, which were not further altered by APAP treatment (Fig. 3B, panels c–f). These aberrant multimembrane structures likely originated from the smooth or rough endoplasmic reticulum. We also found that caspase-3 was activated in Alb-Cre-positive Atg5 Flox/Flox mouse liver which was slightly increased by APAP treatment but not statistically significant (Figs. 3C and 3D), these results were in agreement with the increased basal apoptosis in Alb-Cre-positive Atg5 Flox/Flox mouse liver from HE and TUNEL staining assays (Figs. 2C and 2D). In contrast, there was no caspase activation in APAP-treated Alb-Cre-negative Atg5 Flox/Flox mouse liver, which is in line with the necrotic cell death nature in wild-type mice as we previously reported (Ni *et al*., 2012; Saito *et al*., 2010).

Persistent Activation of Nrf2 Increases Basal Hepatic GSH Content and GSH Recovery as well as Decreases APAP Protein Adduct Formation in Alb-Cre-Positive Atg5 Flox/Flox Mouse Liver

Because Nrf2 was persistently activated in mouse livers with the loss of Atg7 (Komatsu *et al*., 2010), we next determined whether there was a persistent activation of Nrf2 as well as

←

FIG. 2. Mice with the loss of Atg5 are resistant to APAP-induced liver injury. Two-month-old Cre-negative and Cre-positive Atg5 Flox/Flox mice were injected with saline or APAP (500 mg/kg) for 0, 0.5, 2, 6, and 24 h. Serum ALT levels (A) and ratio of the liver to body weight (B) were determined. Data are means ± SE ($n \geq 3$). *$p < 0.05$. One-way ANOVA analysis with Scheffé's *post hoc* test. (C) Cre-negative and Cre-positive Atg5 Flox/Flox mice were injected with saline or APAP (500 mg/kg) for 6 h. Representative photographs of hematoxylin and eosin staining are presented. Panels a–c: Cre-negative Atg5 Flox/Flox mice. Panels d–f: Cre-positive Atg5 Flox/Flox mice. Dotted area in panel b: centrilobular necrosis. Arrow: necrotic cells. Arrow heads: apoptotic cells. Panels c and f were enlarged photographs from panels b and e, respectively. (D) Cre-negative and Cre-positive Atg5 Flox/Flox mice were injected with saline or APAP (500 mg/kg) for 6 h. Representative photographs of TUNEL staining are presented. (E) The number of TUNEL-positive nuclei and total nuclei were quantified from three random fields of three different mice. Data are presented as means ± SE ($n = 3$). *$p < 0.05$. One-way ANOVA analysis with Scheffé's *post hoc* test.

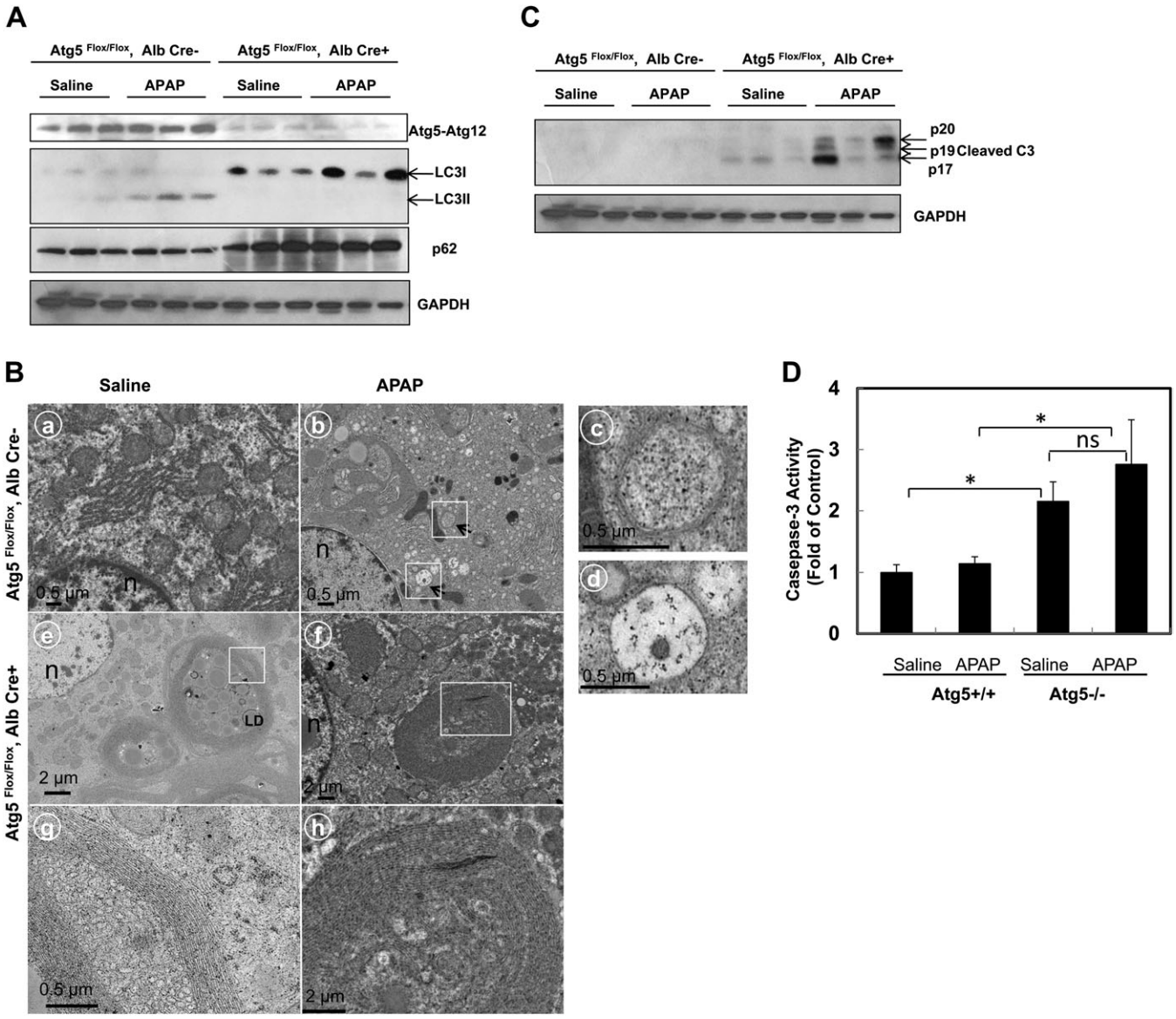

FIG. 3. Lack of LC3-lipidation and autophagosome formation in APAP-treated Cre-positive Atg5 Flox/Flox mouse liver. (A) Cre-negative and Cre-positive Atg5 Flox/Flox mice were injected with saline or APAP (500 mg/kg) for 6 h. Total liver lysates were subjected to Western blot analysis. (B) Mice were treated as in (A), and liver samples were processed for EM. Panels a–d: Cre-negative Atg5 Flox/Flox mice. Panels: e–h: Cre-positive Atg5 Flox/Flox mice. Panels a and e: saline; panels b and f: APAP; panels c and d were from the boxed area in panel b showing representative images of autophagosomes. Panels g and h were from the boxed area from panels e and f, respectively, showing abnormal concentric membranous structures in the Atg5-deficient cells. Arrows denote autophagosomes. LD, lipid droplets; n, nucleus. (C) Mice were treated as in (A), and total liver lysates were subjected to Western blot analysis for cleaved caspase-3 and (D) for caspase-3 activity assay as described in the Materials and Methods section. Data are presented as means ± SE ($n \geq 3$). *$p < 0.05$. One-way ANOVA analysis with Scheffé's *post hoc* test. ns, no statistical significance.

a change in the hepatic GSH content in Alb-Cre-positive Atg5 Flox/Flox mouse livers. Indeed, we found that several Nrf2 target genes including NQO1, GCLM, and GCLC were increased both in messenger RNA (mRNA) and protein levels in Alb-Cre-positive Atg5 Flox/Flox mouse livers, whereas there was no difference in hepatic mRNA expression of Nrf2 and Keap1 between Alb-Cre-positive and -negative Atg5 Flox/Flox mouse livers (Figs. 4A and 4B). Interestingly, we also found that the expression of CYP2E1 was significantly lower in Alb-Cre-positive Atg5 Flox/Flox mouse livers compared with Alb-Cre-negative Atg5 Flox/Flox mouse livers although the mechanisms behind this was not clear (Fig. 4B). It is known that metabolism of APAP results in a rapid loss of hepatic GSH content, and CYP2E1 plays an important role in APAP metabolism. We next determined hepatic GSH levels in these mice and found that the basal hepatic GSH content in the

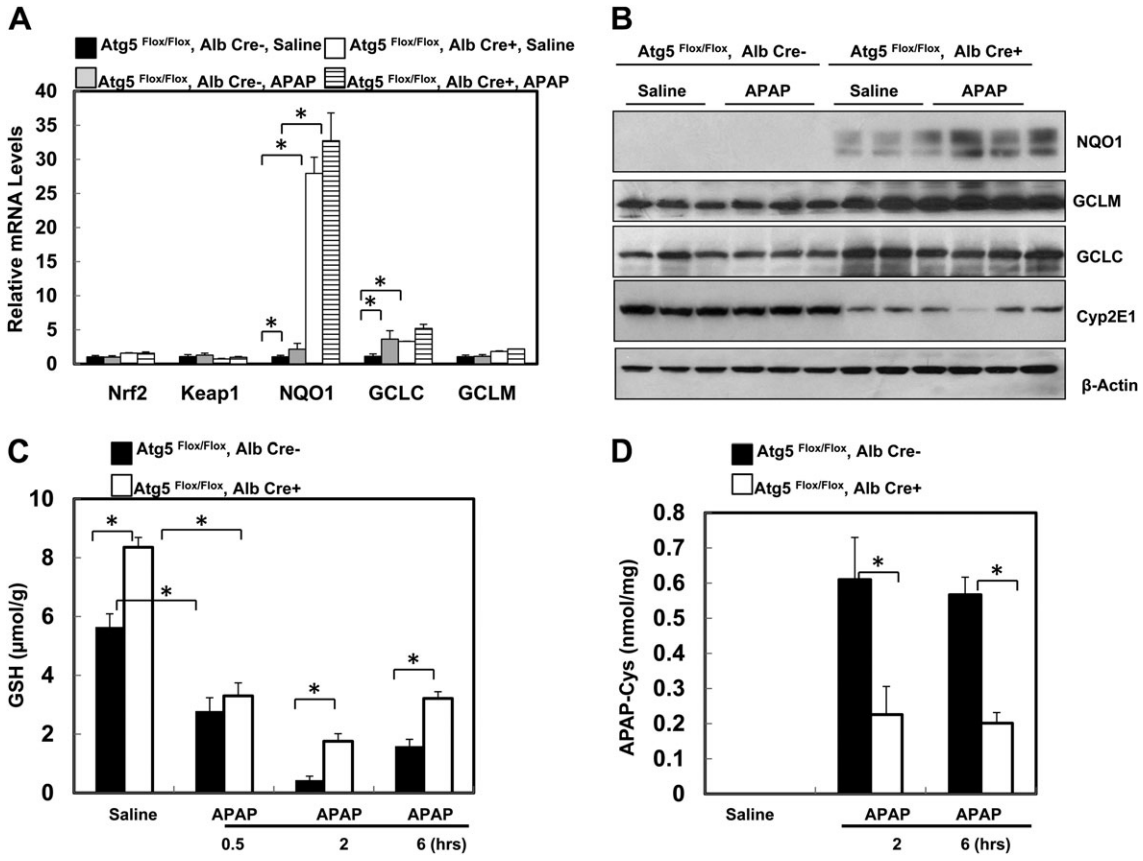

FIG. 4. Loss of Atg5 leads to persistent activation of Nrf2 and increased basal hepatic GSH contents and GSH recovery in the mouse liver. (A) Two-month-old male Cre-negative and Cre-positive Atg5 Flox/Flox mice were injected with saline or APAP (500 mg/kg) for 6 h. Hepatic mRNA was isolated, and real-time reverse transcriptase-PCR was performed as described in the Materials and Methods section. Data are presented as means ± SE ($n = 3$). *$p < 0.05$. One-way ANOVA analysis with Scheffé's *post hoc* test. (B) Mice were treated as in (A), and total liver lysates were subjected to Western blot analysis for NQO1, GCLM, GCLC, and Cyp2E1. (C and D) Mice were treated as in (A), and total hepatic GSH contents (C) and APAP-protein adducts (D) were determined. Data are presented as means ± SE ($n = 3$–6). *$p < 0.05$. One-way ANOVA analysis with Scheffé's *post hoc* test. (E) Two-month-old Cre-negative and Cre-positive Atg5 Flox/Flox mice were injected with corn oil or phorone (100 mg/kg) for 2 h, and hepatic GSH contents were determined. Data are presented as means ± SE ($n = 3$). Mice were pretreated with corn oil or phorone (100 mg/kg) for 2 h followed by treatment either with saline or APAP (500 mg/kg) for another 6 h, and serum ALT levels (F) were determined, representative HE staining images (G) are shown (squared area is enlarged showing an apoptotic cell), and hepatic GSH contents (H) were determined. Data are presented as means ± SE ($n = 3$–6). *$p < 0.05$. One-way ANOVA analysis with Scheffé's *post hoc* test.

untreated Alb-Cre-positive Atg5 Flox/Flox mice was significantly higher than that of Alb-Cre-negative Atg5 Flox/Flox mice (Fig. 4C). At 0.5 h after administration of APAP, the hepatic GSH content was depleted by 50% in both Alb-Cre-positive and Alb-Cre-negative Atg5 Flox/Flox mice (Fig. 4C). In fact, the loss of GSH (as measure of reactive metabolite formation) was more extensive in the Alb-Cre-positive Atg5 Flox/Flox mice suggesting that despite reduced Cyp2E1 protein levels NAPQI is being formed at the same or even higher rate as in control animals. APAP administration reduced GSH levels to 0.4 μmol/g liver in Alb-Cre-negative Atg5 Flox/Flox mice at 2 h followed by a moderate recovery at 6 h (Fig. 4C). In contrast, in Alb-Cre-positive Atg5 Flox/Flox mice, GSH levels were depleted to 1.8 μmol/g liver at 2 h followed by a further recovery at 6 h (Fig. 4C). Although APAP caused an extensive reduction of the hepatic GSH content in Alb-Cre-positive Atg5 Flox/Flox mice, the tissue GSH levels did not reach the same low levels and recovered faster than in Alb-Cre-negative Atg5 Flox/Flox mice. As a consequence of the higher hepatic GSH levels and thus improved detoxification capacity in Alb-Cre-positive Atg5 Flox/Flox mice, the protein adduct levels in these animals were significantly lower at 2 and 6 h after APAP compared with Alb-Cre-negative Atg5 Flox/Flox mice (Fig. 4D).

To investigate whether the higher basal GSH levels or the faster recovery of the GSH contents determines the resistance against APAP-induced liver injury in Alb-Cre-positive Atg5 Flox/Flox mice, animals were treated with phorone to reduce the GSH contents (Jaeschke *et al.*, 1987). After 2 h pretreatment with phorone, mice were treated with APAP for another 6 h. We found that although GSH contents in Alb-Cre-positive Atg5 Flox/Flox mice were reduced to a level almost identical to the Alb-Cre-negative Atg5 Flox/Flox mice (Fig. 4E), phorone plus APAP treatment neither further increased

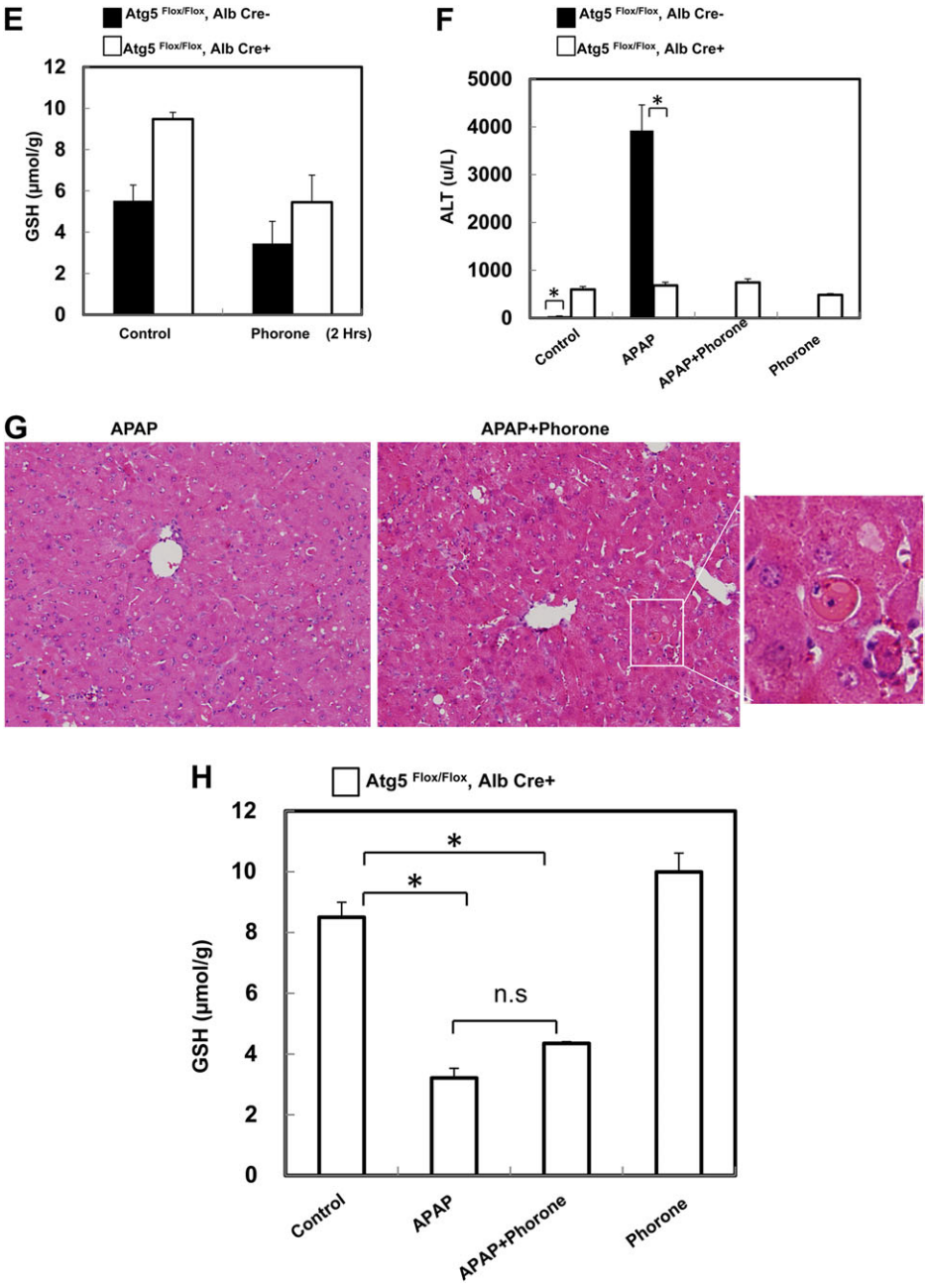

FIG. 4. Continued

serum ALT levels nor altered the liver histology changes. Apoptotic cells but no centrilobular necrosis were detected, which was similar to APAP alone–treated Alb-Cre-positive Atg5 Flox/Flox mice (Fig. 4F–G). Furthermore, phorone pretreatment did not affect the GSH recovery after 6 h treatment with APAP in Alb-Cre-positive Atg5 Flox/Flox mice (Fig. 4H). In addition, the GSH contents in phorone-treated Alb-Cre-positive Atg5 Flox/Flox mice were completely recovered after 8 h (Fig. 4H). Thus, these data suggest that the fast recovery of GSH contents due to the high levels of GSH synthesis enzymes rather than the basal high level of GSH contents in Alb-Cre-positive Atg5 Flox/Flox mice seems play a role in the reduced liver injury in APAP-treated Alb-Cre-positive Atg5 Flox/Flox mice.

Increased Hepatocyte Proliferation in Alb-Cre-Positive Atg5 Flox/Flox Mouse Livers

In response to liver injury, liver has the capacity to regenerate and repair the injury by compensatory hepatocytes proliferation (Michalopoulos and DeFrances, 1997). Because

we observed increased apoptosis in the Alb-Cre-positive Atg5 Flox/Flox mouse liver, we next determined hepatocyte proliferation by using immunostaining and immunoblotting for the cell proliferation marker PCNA. Results from the immunostaining revealed that few PCNA-positive cells were detected in Alb-Cre-negative Atg5 Flox/Flox mouse livers after treatment with either saline or APAP for 6 h. In contrast, PCNA-positive cells were readily detected and increased significantly in Alb-Cre-positive Atg5 Flox/Flox mouse liver compared with Alb-Cre-negative Atg5 Flox/Flox mouse (Figs. 5A and 5B), indicating increased hepatocyte proliferation in the mouse livers that have the loss of Atg5. The increased hepatocyte proliferation in the Alb-Cre-positive Atg5 Flox/Flox mouse liver was not altered after APAP treatment for 6 h but was further increased after APAP treatment for 24 h (Figs. 5A and 5B). After treatment with APAP for 24 h, the number of PCNA-positive cells was also increased in Cre-negative Atg5 Flox/Flox mouse livers. These results were further confirmed by the increased protein levels of PCNA in the Alb-Cre-positive Atg5 Flox/Flox mouse livers (Fig. 5C). We next determined the expression levels of hepatic TNF-α and IL-6 because both cytokines have been implicated in hepatocyte proliferation and liver regeneration. We found that the hepatic mRNA level of TNF-α was almost 10-fold higher, and IL-6 was about twofold higher in the Alb-Cre-positive Atg5 Flox/Flox mouse livers compared with Alb-Cre-negative Atg5 Flox/Flox mouse livers. After APAP treatment, hepatic mRNA levels of TNF-α and IL-6 were further increased in Alb-Cre-positive Atg5 Flox/Flox mouse (Fig. 5D). Taken together, these data suggest that increased hepatocyte proliferation may contribute to the attenuation of APAP-induced liver injury.

DISCUSSION

It has been shown that autophagy protects against cell death by providing nutrients and removing damaged organelles as well as toxic protein aggregates (Mizushima *et al*., 2008). We have previously demonstrated that pharmacological induction of autophagy can protect against APAP-induced liver injury (Ni *et al*., 2012). To our surprise, in the present study, we found that liver-specific Atg5-knockout mice are not more susceptible to APAP-induced liver injury although they already have a higher basal level of apoptosis and mild liver injury. In contrast, liver-specific Atg5-knockout mice are strikingly more resistant to APAP-induced liver injury compared with the matched wild-type mice. The lack of the formation of LC3-PE–conjugated form (LC3-II) and autophagosomes as well as increased p62 protein levels indicate the defects of autophagy in the liver of the mice with the loss of Atg5. The resistance to APAP-induced liver injury in the liver-specific Atg5-knockout mice is likely due to the faster resynthesis of hepatic GSH following APAP administration as a result of persistent activation of Nrf2 as well as compensatory hepatocytes proliferation.

Induction of centrilobular hepatic necrosis has been well documented in APAP overdose–induced liver injury (Hinson *et al*., 2010; Jaeschke and Bajt, 2006). After a therapeutic dose, a large portion of APAP is directly conjugated with glucuronic acid or sulfate through glucuronyl transferase or sulfotransferase and excreted into bile or blood, respectively (Hinson *et al*., 2010; Jaeschke and Bajt, 2006). The remaining part of the dose is metabolized by the hepatic P450 system to generate the reactive NAPQI. After an overdose, the increased NAPQI reacts with GSH to deplete intracellular GSH and thus increases oxidative stress (Jaeschke, 1990; Jaeschke and Bajt, 2006). Once GSH is depleted, NAPQI binds to many cellular and mitochondrial proteins to form protein adducts (Jaeschke and Bajt, 2006). Depletion of intracellular GSH and increased protein adducts (in particular mitochondrial protein adducts) leads to mitochondrial damage and decrease of cellular ATP levels, which have been thought to be the major mechanisms for APAP-induced necrosis (Hinson *et al*., 2010; Jaeschke and Bajt, 2006). It is interesting to note that APAP-induced mitochondrial damage and mitochondrial permeability transition also resulted in the release of cytochrome c and apoptosis-inducing factor from mitochondria, a key event that triggers caspase activation and apoptosis in most scenarios (Jaeschke and Bajt, 2006). However, no convincing evidence has been presented to show the involvement of caspase and apoptosis in the livers of APAP-treated mice (Jaeschke and Bajt, 2006). One possible explanation for the lack of caspase activation in the livers of APAP-treated mice is the APAP-induced depletion of cellular ATP because ATP is required for the activation of caspase (Jaeschke and Bajt, 2006). Although preventing APAP-induced necrosis and enhancing ATP levels by glycine and fructose eventually triggered apoptosis in cultured hepatocytes (Kon *et al*., 2004), the concept that declining ATP levels is the reason for lack of apoptosis could not be confirmed *in vivo* (Williams *et al*., 2011).

Autophagy and cell death are intimately connected, although the relationship between autophagy and cell death has been hotly debated recently. However, there are numerous conditions, in which autophagy acts as a cell survival process. Genetic deletion of key autophagy genes, such as Atg3, Atg5 and Atg7, all result in premature death of newborn mice (Mizushima, 2011). Liver-specific knockout Atg7 leads to severe liver injury (Komatsu *et al*., 2010) although the cell death nature in these mice was not known. In the present study, we found increased caspase activation and apoptosis in the livers of Atg5-knockout mice (Fig. 2), suggesting that liver injury in the autophagy-deficient mouse livers could be due to increased apoptosis. At the cellular level, pharmacological inhibition of autophagy or siRNA knockdown of essential autophagy genes all lead to more apoptotic cell death when cells are deprived of growth factors or other stresses (Ding *et al*., 2007; Lum *et al*., 2005). Moreover, we recently found that activation of autophagy can also protect against APAP-induced necrosis (Ni *et al*., 2012). Thus, it is clear that

autophagy can serve as a protective mechanism against both apoptosis and necrosis. However, in some circumstances, autophagy seems to promote cell death, termed autophagic cell death (Shimizu *et al*., 2004). We do not think that APAP caused autophagic cell death because activation of autophagy by rapamycin suppresses APAP-induced liver injury (Ni *et al*., 2012). The decreased liver injury in APAP-treated mouse livers with the loss of Atg5 is not directly due to the lack of autophagy but rather due to the secondary compensatory effects (see below).

It should be noted that although autophagy can regulate cell death, apoptosis in particular can also affect autophagic processes. Caspase activation can suppress autophagy by the cleavage of Beclin 1 (Mei *et al*., 2011), an essential autophagy gene in the regulation of the autophagy induction. Therefore, autophagy, apoptosis, and necrosis are intimately connected, and it seems in most cases that autophagy can protect against apoptosis and necrosis, whereas apoptosis can inhibit autophagy.

We have previously reported that pharmacological inhibition of lysosomal degradation by chloroquine exacerbated, whereas induction of autophagy by rapamycin almost completely inhibited, APAP-induced liver injury (Ni *et al*., 2012). This seems paradoxical because if autophagy can protect against cell death, why would the mice with liver-specific deletion of Atg5 be more resistant to APAP-induced liver injury? However, genetic knockout of Atg5 in the mouse liver is a chronic process that may result in cellular compensatory responses. Indeed, knockout of Atg7 in the mouse liver leads to hepatomegaly and persistent activation of Nrf2 due to the accumulation of p62, a protein that is normally degraded by autophagy (Komatsu *et al*., 2010). We found similar results in the mice with the liver-specific deletion of Atg5, suggesting that hepatomegaly and activation of Nrf2 could be general phenomena during chronic suppression of autophagy in the liver. It has been shown that Nrf2-knockout mice are more susceptible, whereas liver-specific Keap1-knockout mice, which have persistent activation of Nrf2, are more resistant to APAP-induced liver injury (Reisman *et al*., 2009). Nrf2 is a transcription factor critical for protection against electrophilic and oxidative stress by regulating the expression of many cytoprotective genes, such as NQO1, GCLC, and GCLM. Both GCLC and GCLM are key enzymes that regulate hepatic GSH synthesis. Indeed, we found that both enzymes were highly upregulated in the mouse livers that had the loss of Atg5. As a result, we found a higher basal GSH content in these mice and a higher recovery rate of GSH in Atg5-deficient mouse livers than that of wild-type animals. However, when the basal GSH content was reduced to the same level as in wild-type animals, APAP still did not cause any injury, suggesting that the protection was not dependent on the initially higher GSH levels. Moreover, we also found that the decreased Cyp2E1 expression did not affect the bioactivation of APAP in Atg5-deficient mouse livers based on the observation that the loss of GSH during the first 30 min after treatment as a marker for metabolic activation was not attenuated in Atg5-deficient mice. This indicates that either the lower level of Cyp2E1 is sufficient or other P450 enzymes may be involved in the metabolism of APAP in Atg5-deficient mouse liver. However, given the fact that Atg5-deficient mice showed lower levels of protein adducts, the data are consistent with the hypothesis that the higher rates of GSH synthesis prevented complete GSH depletion, attenuated protein binding, and ultimately eliminated the initiation of the intracellular signaling cascade leading to cell necrosis. Taken together, the faster recovery rate of GSH in Atg5-deficient mouse liver as a result of persistent activation of Nrf2 may be an important mechanism against APAP-induced liver injury.

A recent paper by Igusa *et al*. (2012) reported that APAP treatment enhanced of liver injury in Atg7-deficient mice by induction of apoptosis. Deletion of Atg7 was achieved by treatment with poly(inosinic acid)-poly(cytidylic acid) (pIpC). pIpC can first inhibit and later induce P450 enzyme activities and affect APAP bioactivation and hepatotoxicity (Kalabis and Wells, 1990). Because the bioactivation of APAP was not assessed in that study, the mechanisms for the increased liver injury in APAP-treated Atg7-deficient mice were not clear. Moreover, the persistent activation of Nrf2 and its role in APAP-induced liver injury in the Atg7-deficient mice were also not determined in that study. Because of the increasing interests in autophagy research and the use of autophagy gene knockout mice, our results indicate that caution must be taken when using these mice to assess APAP hepatotoxicity because the compensatory events needs to be taken into consideration for the data interpretation.

The liver is a unique organ that has a remarkable capacity to regenerate after injury. The necrotic cells induced by APAP exposure can be replaced by the proliferating hepatocytes, and it has been found that the most extensively proliferating hepatocytes are located in the transition zone between necrotic and healthy cells (Bajt *et al*., 2003). Although the regeneration process is very complicated, it has been suggested that the priming of hepatocytes by cytokines, such as TNF-α and IL-6, makes the hepatocytes more responsive to growth factors and encourages proliferation. After APAP treatment, liver regeneration was impaired in IL-6-knockout and in TNF receptor type I–knockout mice (Chiu *et al*., 2003; James *et al*., 2003). In this study, we found that the basal levels of TNF-α and IL-6 in the mouse livers with the loss of Atg5 are significantly higher than that of the wild-type mice. Moreover, the cell cycle proteins, such as cyclin D and cyclin E, were also elevated in the mouse livers with the loss of Atg5 (Ni and Ding, unpublished data). All these factors may contribute to the increased hepatocyte proliferation in mouse livers with loss of Atg5, which may also attenuate APAP-induced liver injury by increasing the capacity of liver repair.

In conclusion, we have demonstrated that mice with the liver-specific loss of Atg5 are more resistant to APAP-induced liver injury. The striking resistance to APAP-induced liver injury is likely due to the persistent activation of Nrf2 and

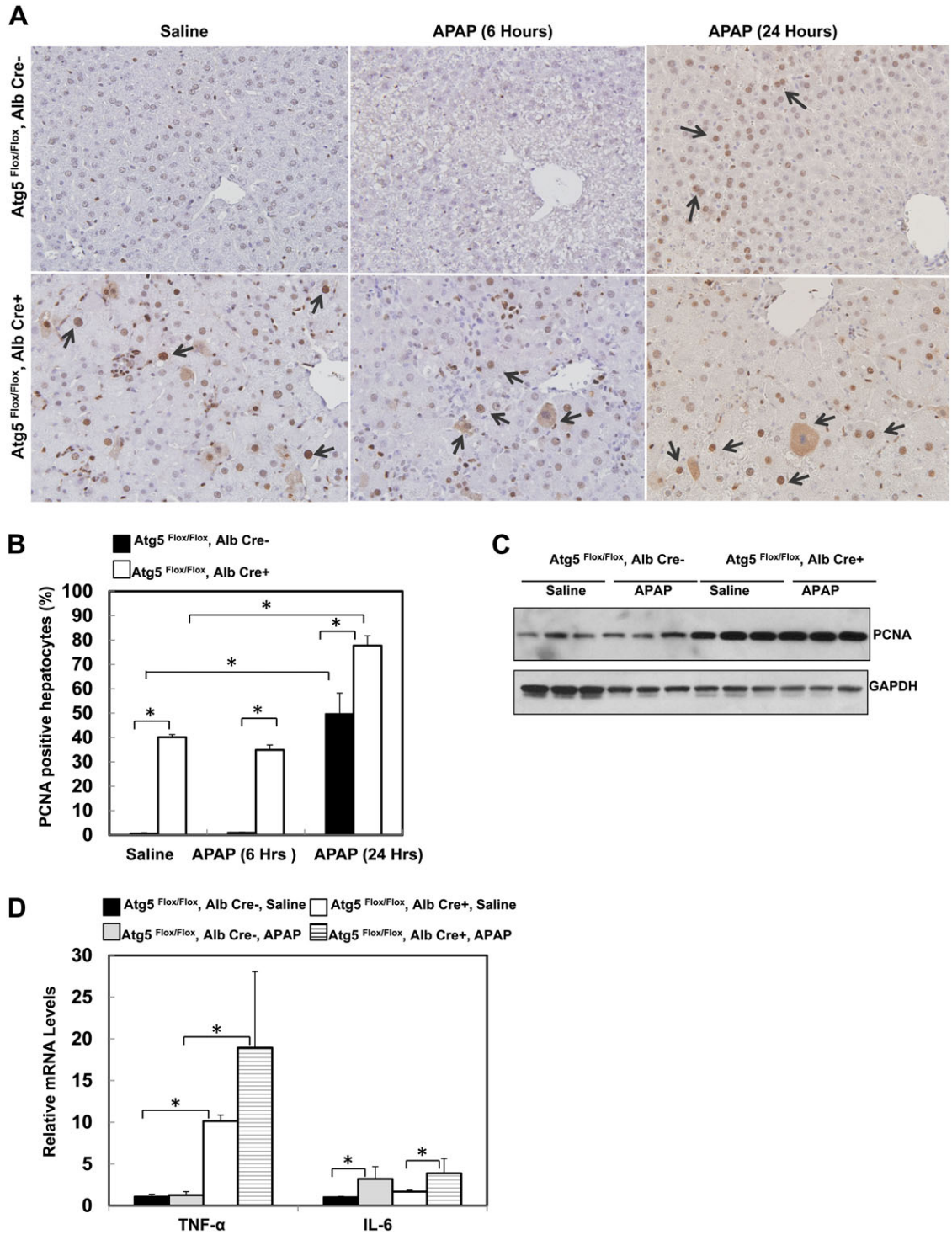

FIG. 5. Loss of Atg5 leads to compensatory hepatocyte proliferation in the mouse liver. (A) Two-month-old male Cre-negative and Cre-positive Atg5 Flox/Flox mice were injected with saline or APAP (500 mg/kg) for 6 and 24 h. Tissue sections were subjected to immunostaining for PCNA. Arrows: representative PCNA-positive cells. (B) The number of PCNA-positive nuclei and total nuclei were quantified from three random fields of three different mice. Data are presented as means ± SE ($n = 3$). *$p < 0.05$. One-way ANOVA analysis with Scheffé's *post hoc* test. (C) Mice were treated as in (A) for 6 h, and total liver lysates were subjected to Western blot analysis for PCNA. (D) Two-month-old male Cre-negative and Cre-positive Atg5 Flox/Flox mice were injected with saline or APAP (500 mg/kg) for 6 h. Hepatic mRNA was isolated, and real-time reverse transcriptase-PCR was performed as described in the Materials and Methods section. Data are presented as means ± SE ($n = 3$). *$p < 0.05$. One-way ANOVA analysis with Scheffé's *post hoc* test.

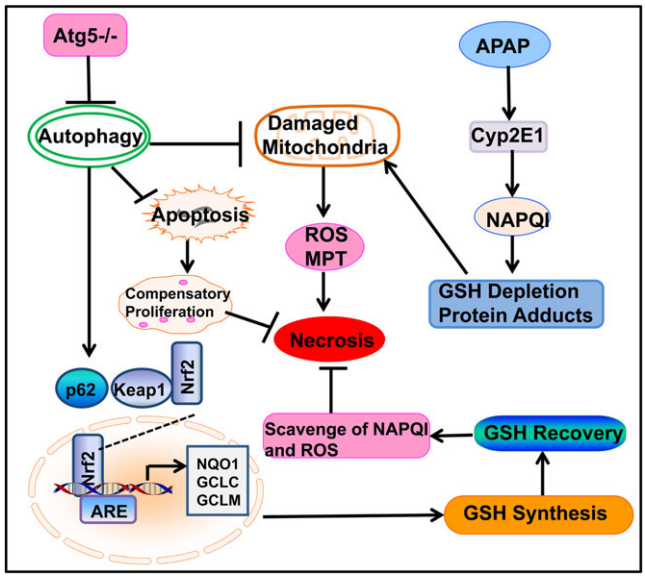

FIG. 6. A proposed model for the loss of Atg5 in the mouse liver and the cross talk among autophagy, apoptosis, and necrosis in APAP-induced liver injury. In APAP-treated hepatocytes, APAP is first metabolized through the cytochrome P450 enzymes (mainly via CYP2E1) and generates reactive metabolites that bind to cellular and mitochondrial proteins to initiate mitochondrial damage. Damaged mitochondria can lead to necrotic cell death by inducing onset of mitochondria permeability transition (MPT) and reactive oxygen species (ROS) production. Genetic deletion of Atg5 in the mouse liver leads to the suppression of autophagy and accumulation of p62. Increased p62 proteins results in persistent activation of Nrf2 in the mouse liver by releasing the inhibition of Keap1 on Nrf2. Persistent activation of Nrf2 increases the expression of GSH synthesis enzymes, resulting in the increased recovery of GSH content in the mouse liver that further scavenges NAPQI and ROS to protect against APAP-induced liver injury. Loss of autophagy may increase the baseline hepatocytes apoptosis in the mouse liver resulting in compensatory proliferation, which may also attenuate APAP-induced liver injury by promoting liver repair and regeneration.

increased hepatocyte proliferation. The cellular and molecular events regulating necrosis, apoptosis, and autophagy in the liver-specific Atg5-knockout mice after exposure to APAP are summarized in Figure 6.

FUNDING

National Institute of Health (NIH) funds (R01 AA020518-01, R21 AA017421, P20 RR021940, and P20 RR016475) from the INBRE program of the National Center for Research Resources (W.X.D). H.J. was supported by the NIH funds (R01 DK070195).

REFERENCES

Bajt, M. L., Farhood, A., Lemasters, J. J., and Jaeschke, H. (2008). Mitochondrial bax translocation accelerates DNA fragmentation and cell necrosis in a murine model of acetaminophen hepatotoxicity. *J. Pharmacol. Exp. Ther.* **324,** 8–14.

Bajt, M. L., Knight, T. R., Farhood, A., and Jaeschke, H. (2003). Scavenging peroxynitrite with glutathione promotes regeneration and enhances survival during acetaminophen-induced liver injury in mice. *J. Pharmacol. Exp. Ther.* **307,** 67–73.

Chiu, H., Gardner, C. R., Dambach, D. M., Durham, S. K., Brittingham, J. A., Laskin, J. D., and Laskin, D. L. (2003). Role of tumor necrosis factor receptor 1 (p55) in hepatocyte proliferation during acetaminophen-induced toxicity in mice. *Toxicol. Appl. Pharmacol.* **193,** 218–227.

Corcoran, G. B., Racz, W. J., Smith, C. V., and Mitchell, J. R. (1985). Effects of N-acetylcysteine on acetaminophen covalent binding and hepatic necrosis in mice. *J. Pharmacol. Exp. Ther.* **232,** 864–872.

Cover, C., Mansouri, A., Knight, T. R., Bajt, M. L., Lemasters, J. J., Pessayre, D., and Jaeschke, H. (2005). Peroxynitrite-induced mitochondrial and endonuclease-mediated nuclear DNA damage in acetaminophen hepatotoxicity. *J. Pharmacol. Exp. Ther.* **315,** 879–887.

Ding, W. X., Ni, H. M., DiFrancesca, D., Stolz, D. B., and Yin, X. M. (2004). Bid-dependent generation of oxygen radicals promotes death receptor activation-induced apoptosis in murine hepatocytes. *Hepatology* **40,** 403–413.

Ding, W. X., Ni, H. M., Gao, W., Chen, X., Kang, J. H., Stolz, D. B., Liu, J., and Yin, X. M. (2009). Oncogenic transformation confers a selective susceptibility to the combined suppression of the proteasome and autophagy. *Mol. Cancer Ther.* **8,** 2036–2045.

Ding, W. X., Ni, H. M., Gao, W., Hou, Y. F., Melan, M. A., Chen, X., and Yin, X. M. (2007). Differential effects of endoplasmic reticulum stress-induced autophagy on cell survival. *J. Biol. Chem.* **282,** 4702–4710.

Hanawa, N., Shinohara, M., Saberi, B., Gaarde, W. A., Han, D., and Kaplowitz, N. (2008). Role of JNK translocation to mitochondria leading to inhibition of mitochondria bioenergetics in acetaminophen-induced liver injury. *J. Biol. Chem.* **283,** 13565–13577.

Hara, T., Nakamura, K., Matsui, M., Yamamoto, A., Nakahara, Y., Suzuki-Migishima, R., Yokoyama, M., Mishima, K., Saito, I., Okano, H., and Mizushima, N. (2006). Suppression of basal autophagy in neural cells causes neurodegenerative disease in mice. *Nature* **441,** 885–889.

Hinson, J. A., Roberts, D. W., and James, L. P. (2010). Mechanisms of acetaminophen-induced liver necrosis. *Handb. Exp. Pharmacol.* **196,** 369–405.

Igusa, Y., Yamashina, S., Izumi, K., Inami, Y., Fukada, H., Komatsu, M., Tanaka, K., Ikejima, K., and Watanabe, S. (2012). Loss of autophagy promotes murine acetaminophen hepatotoxicity. *J. Gastroenterol.* **47,** 433–443.

Inami, Y., Waguri, S., Sakamoto, A., Kouno, T., Nakada, K., Hino, O., Watanabe, S., Ando, J., Iwadate, M., Yamamoto, M., *et al.* (2011). Persistent activation of Nrf2 through p62 in hepatocellular carcinoma cells. *J. Cell Biol.* **193,** 275–284.

Jaeschke, H. (1990). Glutathione disulfide formation and oxidant stress during acetaminophen-induced hepatotoxicity in mice in vivo: The protective effect of allopurinol. *J. Pharmacol. Exp. Ther.* **255,** 935–941.

Jaeschke, H., and Bajt, M. L. (2006). Intracellular signaling mechanisms of acetaminophen-induced liver cell death. *Toxicol. Sci.* **89,** 31–41.

Jaeschke, H., Kleinwaechter, C., and Wendel, A. (1987). The role of acrolein in allyl alcohol-induced lipid peroxidation and liver cell damage in mice. *Biochem. Pharmacol.* **36,** 51–57.

Jaeschke, H., Knight, T. R., and Bajt, M. L. (2003). The role of oxidant stress and reactive nitrogen species in acetaminophen hepatotoxicity. *Toxicol. Lett.* **144,** 279–288.

James, L. P., Lamps, L. W., McCullough, S., and Hinson, J. A. (2003). Interleukin 6 and hepatocyte regeneration in acetaminophen toxicity in the mouse. *Biochem. Biophys. Res. Commun.* **309,** 857–863.

Kalabis, G. M., and Wells, P. G. (1990). Biphasic modulation of acetaminophen bioactivation and hepatotoxicity by pretreatment with the

interferon inducer polyinosinic-polycytidylic acid. *J. Pharmacol. Exp. Ther.* **255,** 1408–1419.

Knight, T. R., Ho, Y. S., Farhood, A., and Jaeschke, H. (2002). Peroxynitrite is a critical mediator of acetaminophen hepatotoxicity in murine livers: Protection by glutathione. *J. Pharmacol. Exp. Ther.* **303,** 468–475.

Komatsu, M., Kurokawa, H., Waguri, S., Taguchi, K., Kobayashi, A., Ichimura, Y., Sou, Y. S., Ueno, I., Sakamoto, A., Tong, K. I., *et al.* (2010). The selective autophagy substrate p62 activates the stress responsive transcription factor Nrf2 through inactivation of Keap1. *Nat. Cell Biol.* **12,** 213–223.

Komatsu, M., Waguri, S., Ueno, T., Iwata, J., Murata, S., Tanida, I., Ezaki, J., Mizushima, N., Ohsumi, Y., Uchiyama, Y., *et al.* (2005). Impairment of starvation-induced and constitutive autophagy in Atg7-deficient mice. *J. Cell Biol.* **169,** 425–434.

Kon, K., Kim, J. S., Jaeschke, H., and Lemasters, J. J. (2004). Mitochondrial permeability transition in acetaminophen-induced necrosis and apoptosis of cultured mouse hepatocytes. *Hepatology* **40,** 1170–1179.

Kuma, A., Hatano, M., Matsui, M., Yamamoto, A., Nakaya, H., Yoshimori, T., Ohsumi, Y., Tokuhisa, T., and Mizushima, N. (2004). The role of autophagy during the early neonatal starvation period. *Nature* **432,** 1032–1036.

Larson, A. M., Polson, J., Fontana, R. J., Davern, T. J., Lalani, E., Hynan, L. S., Reisch, J. S., Schiodt, F. V., Ostapowicz, G., Shakil, A. O., *et al.* (2005). Acetaminophen-induced acute liver failure: Results of a United States multicenter, prospective study. *Hepatology* **42,** 1364–1372.

Lum, J. J., Bauer, D. E., Kong, M., Harris, M. H., Li, C., Lindsten, T., and Thompson, C. B. (2005). Growth factor regulation of autophagy and cell survival in the absence of apoptosis. *Cell* **120,** 237–248.

McGill, M. R., Yan, H. M., Ramachandran, A., Murray, G. J., Rollins, D. E., and Jaeschke, H. (2011). HepaRG cells: A human model to study mechanisms of acetaminophen hepatotoxicity. *Hepatology* **53,** 974–982.

Mei, S., Ni, H. M., Manley, S., Bockus, A., Kassel, K. M., Luyendyk, J. P., Copple, B., and Ding, W. X. (2011). Differential roles of unsaturated and saturated fatty acids on autophagy and apoptosis in hepatocytes. *J. Pharmacol. Exp. Ther.* **393,** 497–498.

Meyers, L. L., Beierschmitt, W. P., Khairallah, E. A., and Cohen, S. D. (1988). Acetaminophen-induced inhibition of hepatic mitochondrial respiration in mice. *Toxicol. Appl. Pharmacol.* **93,** 378–387.

Michalopoulos, G. K., and DeFrances, M. C. (1997). Liver regeneration. *Science* **276,** 60–66.

Mitchell, J. R., Jollow, D. J., Potter, W. Z., Davis, D. C., Gillette, J. R., and Brodie, B. B. (1973). Acetaminophen-induced hepatic necrosis. I. Role of drug metabolism. *J. Pharmacol. Exp. Ther.* **187,** 185–194.

Mizushima, N. (Forthcoming). Autophagy in protein and organelle turnover. *Cold Spring Harb. Symp. Quant. Biol.*

Mizushima, N., Levine, B., Cuervo, A. M., and Klionsky, D. J. (2008). Autophagy fights disease through cellular self-digestion. *Nature* **451,** 1069–1075.

Muldrew, K. L., James, L. P., Coop, L., McCullough, S. S., Hendrickson, H. P., Hinson, J. A., and Mayeux, P. R. (2002). Determination of acetaminophen-protein adducts in mouse liver and serum and human serum after hepatotoxic doses of acetaminophen using high-performance liquid chromatography with electrochemical detection. *Drug Metab. Dispos.* **30,** 446–451.

Ni, H. M., Bockus, A., Boggess, N., Jaeschke, H., and Ding, W. X. (2012). Activation of autophagy protects against acetaminophen-induced hepatotoxicity. *Hepatology* **55,** 222–232.

Ohsumi, Y., and Mizushima, N. (2004). Two ubiquitin-like conjugation systems essential for autophagy. *Semin. Cell Dev. Biol.* **15,** 231–236.

Reisman, S. A., Csanaky, I. L., Aleksunes, L. M., and Klaassen, C. D. (2009). Altered disposition of acetaminophen in Nrf2-null and Keap1-knockdown mice. *Toxicol. Sci.* **109,** 31–40.

Saito, C., Zwingmann, C., and Jaeschke, H. (2010). Novel mechanisms of protection against acetaminophen hepatotoxicity in mice by glutathione and N-acetylcysteine. *Hepatology* **51,** 246–254.

Shimizu, S., Kanaseki, T., Mizushima, N., Mizuta, T., Arakawa-Kobayashi, S., Thompson, C. B., and Tsujimoto, Y. (2004). Role of Bcl-2 family proteins in a non-apoptotic programmed cell death dependent on autophagy genes. *Nat. Cell Biol.* **6,** 1221–1228.

Takamura, A., Komatsu, M., Hara, T., Sakamoto, A., Kishi, C., Waguri, S., Eishi, Y., Hino, O., Tanaka, K., and Mizushima, N. (2011). Autophagy-deficient mice develop multiple liver tumors. *Genes Dev.* **25,** 795–800.

Williams, C. D., Koerner, M. R., Lampe, J. N., Farhood, A., and Jaeschke, H. (2011). Mouse strain-dependent caspase activation during acetaminophen hepatotoxicity does not result in apoptosis or modulation of inflammation. *Toxicol. Appl. Pharmacol.* **257,** 449–458.

Wolfe, A., Thomas, A., Edwards, G., Jaseja, R., Guo, G. L., and Apte, U. (2011). Increased activation of the Wnt/beta-catenin pathway in spontaneous hepatocellular carcinoma observed in farnesoid X receptor knockout mice. *J. Pharmacol. Exp. Ther.* **338,** 12–21.